DETERMINING DETONATION THRESHOLD FOR MULTIPLE FRAGMENT IMPACTS

By Lucia Kuhns and Leonard T. Wilson
Naval Surface Warfare Center, Dahlgren Division, Dahlgren VA

ABSTRACT

Dual fragment impacts were studied using the Eulerian hydrocode CTH. The purposes of the study were to gain insight into the physical phenomena underlying multiple fragment impacts, and to develop an equation that predicts critical fragment velocity, the velocity at which a fragment must travel to cause a detonation in a covered explosive, for dual fragment impacts. Identical steel fragments were used, and the target coverplate material, coverplate thickness, and the energetic material were held constant. The first analysis studied fragment separation in the dimension parallel to the target surface, with zero time separation. The next analysis was conducted varying the time between fragment impacts, with zero distance separation. The next analysis was performed varying the fragment separation in time and in distance simultaneously. Finally, the analysis was extended to other fragment sizes to determine if a general equation could be developed. The analyses showed that the distance separating fragments (in the dimension parallel to the target) can significantly affect the critical velocity required to initiate a covered charge. The effect of separating fragments in time can be even more detrimental to the target than simply placing fragments close together in space. A general critical velocity relation which accounts for variation in impact times may depend on more variables than are easily determined for or employed in an empirical relation.

BACKGROUND

Multiple fragment impact is one of the U.S. Navy's critical insensitive munitions tests. In this test, 250-grain steel fragments are launched against ordnance items. At least two fragments must impact the test item. To pass the test, a burning reaction from the ordnance item is the most violent reaction allowed. The empirical Jacobs-Roslund relation[1] and hydrocode analysis are used to predict the explosive response. The Jacobs-Roslund equation is given by

$$V_c = \frac{A}{\sqrt{d\cos q}}(1+B)\left(1+\frac{CT}{d}\right) \qquad [1]$$

where

V_c is the critical fragment velocity required for a fragment to initiate an explosive charge
A is an empirical constant defining the explosive sensitivity
d is the critical fragment dimension

θ is the fragment obliquity angle
B is the fragment shape coefficient
C is the coverplate protection coefficient
T is the coverplate thickness

However, in many instances, the ordnance item will detonate even though analysis does not predict detonation. Although the shock-to-detonation-transition (SDT) models used in the hydrocodes codes are well understood, there are discrepancies between simulation results and test results. A possible reason for this inconsistency is that fragment impact simulations typically involve a single fragment, while several fragments strike the test object during testing. Similarly, the Jacobs-Roslund equation does not account for the effects of multiple fragment impact either.

To determine whether the simplified modeling could cause the discrepancies, we used the Eulerian hydrocode CTH[2] to study dual fragment impacts. The purpose of the modeling was twofold. First, we wanted to gain insight into the physical phenomena underlying multiple fragment impacts. The second objective of the study was to extend the Jacobs-Roslund relation to account for multiple fragments – to develop an equation that predicts critical fragment velocity, the velocity at which a covered explosive will detonate given dual fragment impacts.

We envisioned the extended Jacobs-Roslund relation as the equation above with an additional scaling factor based on the distance between the fragments.

TECHNICAL APPROACH

When considering dual fragment impacts, there are many variables that affect the results: relative fragment size, shape, and material (are both fragments the same?), absolute fragment size and shape (will results scale with fragment size?), fragment separation distances in two dimensions (in what units should the separations be defined?), target coverplate material and thickness, and the energetic material. To narrow the scope of the effort, we used identical steel fragments and held the target coverplate material, coverplate thickness, and the energetic material constant. The coverplate material is steel, the thickness is 0.3 inch (0.762 cm), and the energetic material is Comp B. We chose Comp B because it is an ideal explosive and well characterized. For this study, five of the six variables upon which the Jacobs-Roslund critical velocity depends are constant; only d is varied.

For our initial case, we used 250-grain platelets, 0.648 inch (1.645 cm) by 0.648 inch by 0.3 inch (0.762 cm) thick. We chose this fragment size because 250-grain fragments are typically used during Multiple Fragment Impact tests. The test fragments are cubes, 0.5 inch (1.27 cm) on a side. We varied the separation between the fragments in two dimensions to find the effect on the critical fragment velocity. The first dimension is parallel to the target surface, measured in fragment diameters (shown in Figure 1), and the second dimension is perpendicular to the target surface, measured in microseconds (time between first and second impacts, shown in Figure 2).

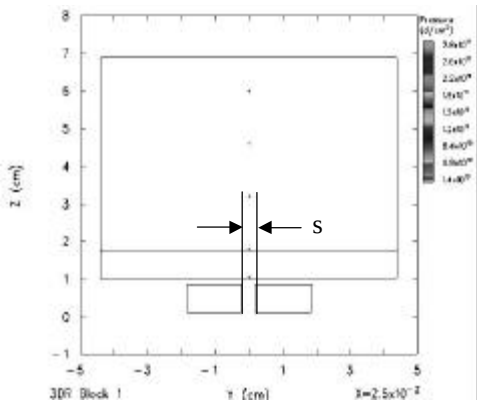

Figure 1. Separation Parallel to Target, s

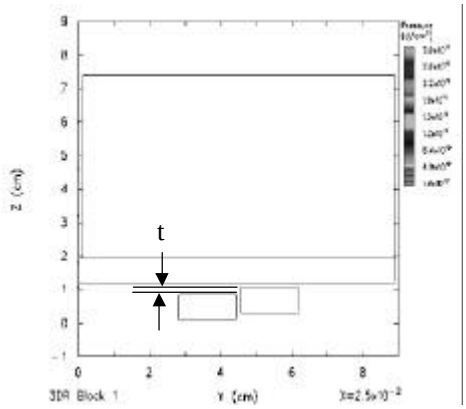

Figure 2. Separation Perpendicular to Target, t

For zero time separation, the hydrocode runs were three-dimensional, with quarter symmetry (symmetric in both x and y, with the x-symmetry plane parallel to the page, through the center of the fragments, and the y-symmetry plane at the centerline between the fragments). The runs involving separation in time were three-dimensional with half symmetry (symmetric in x, with the x-symmetry plane parallel to the page, through the center of the fragments). We estimated the critical velocity and iterated until finding the velocity within 100 ft/s (33 m/s). We fit these data to a surface – a detonation threshold surface. To create a surface that can be used as a scaling function for the Jacobs-Roslund relation we normalized the critical velocities by the single fragment critical velocity. This generated a function with a maximum value of one. Then we attempted to generalize the scaling function by investigating smaller fragment sizes and different shapes (varying the fragment T/d – target coverplate thickness to fragment diameter ratio).

REACTIVE BURN MODEL

CTH uses the History Variable Reactive Burn (HVRB)[3] model to predict a shock-to-detonation transition (SDT). HVRB is a pressure-dependent model based upon the following equations:

$$l = f^M$$

$$f = \frac{1}{t_0}\int_0^t \left(\frac{P - P_i}{P_r} \right)^z dt \qquad [2, 3]$$

where

l is the extent of reaction (0 to 1)
f is a history variable
t_o is a unit time, to non-dimensionalize ϕ
P is the pressure in the material
z is a function of the slope of the Pop plot of the material, related to explosive sensitivity
P_r is the pressure in a wedge test which causes a transition to detonation in 1μs
P_i is a cut off pressure below which pressure contributions are not significant

The history variable is a function of pressure integrated over time, which means that for a given pressure, f increases with time.

RESULTS

Comparison Between Jacobs-Roslund and CTH Predictions

We used the Jacobs-Roslund relation to predict the critical velocity for 250 and 60 grain fragments impacting both bare and covered explosive. For the case of two fragments side by side, we used a modified Jacobs-Roslund relation[1] to account for the irregular shape of an equivalent single fragment. The modified relation – based upon energy principles – uses fragment projected area instead of critical diameter ($A^{1/4}$ instead of $d^{1/2}$, since $A = d^2$ for a square fragment). We extended the modification to the final factor of the Jacobs-Roslund relation, using $A^{1/2}$ instead of d. We then compared the empirical Jacobs-Roslund predictions with CTH predictions to see how closely they agree. The results are shown below in Table 1.

Table 1. Results of Comparison Between Jacobs-Roslund and CTH Predictions

Critical Velocity Comparison	***Covered Explosive***			***Bare Explosive***		
	Jacobs-Roslund (ft/s)	CTH (ft/s)	% difference from J-R	Jacobs-Roslund (ft/s)	CTH (ft/s)	% difference from J-R
60-grain	9207	10150	10.2	3534	4250	20.3
120-grain	6352	6350	0			
250-grain	4424	4150	-6.2	2475	2450	-1.0
2 60-grain*	6345	6850	8.0			
2 120-grain*	4509	4750	5.3			
2 250-grain*	3240	3350	3.4			

* modified Jacobs-Roslund relation

Note from Table 1 that Jacobs-Roslund and CTH vary only about 10 percent for most cases. The only large difference is seen in the case of the 60-grain fragment impacting bare explosive, where the results differ by about 20 percent. The closeness of the predictions indicates that CTH is a reasonable tool to use for studying variations in fragment separation for the purpose of extending the Jacobs-Roslund relation, especially for the 250-grain case.

Studying 250-Grain Fragments

In developing the detonation threshold surface, we first studied separation in the dimension parallel to the target surface, with zero time separation. These results are the most straightforward. For narrow separations, there was interaction between the shock waves generated by each fragment. The resultant detonation wave was centered between the fragments, as shown in Figure 3. This is consistent with the HVRB model, because the two pressure waves sustain each other where they intersect, although the outer ends of the waves experience relief. As a result of the interaction, the critical velocity is lower than that of a single fragment. This is consistent with the Jacobs-Roslund predictions shown in Table 1, where two adjacent fragments are calculated as a single larger fragment. The larger fragment requires less velocity to impart an equivalent amount of energy to the explosive.

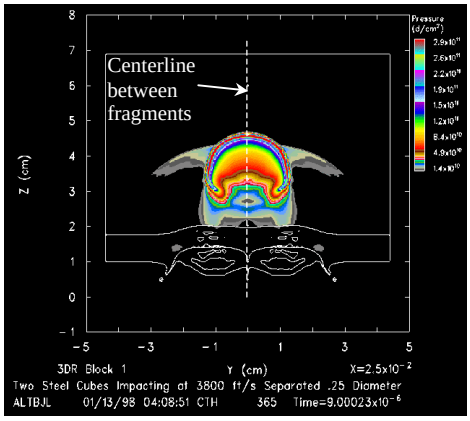

Figure 3. Predicted Detonation between Fragments

The distance between the fragments was increased until the critical velocity steadied at the single fragment critical velocity. At this point, there was no longer a single detonation wave between the two fragments, but separate detonations initiated by each fragment. The results are shown in Figure 4. The data points fit an exponential curve, which we chose using two-dimensional curve-fitting software by Jandel Scientific[4].

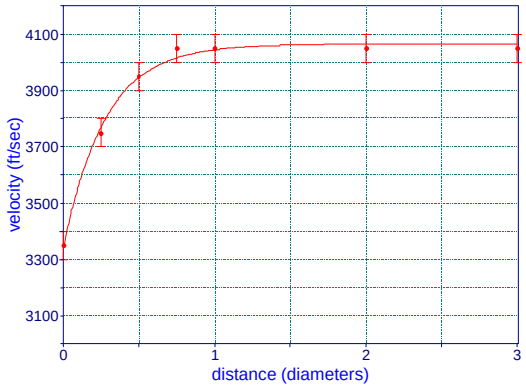

Figure 4. Summary of Zero Time Separation Results for 250-Grain Fragments

The next step in developing the detonation threshold surface was to vary the time between impacts, with zero distance separation. The mechanisms that govern the interaction between fragments spaced in time are more complex than those that govern the interaction between fragments spaced in distance. Detonations due to fragment interaction do not occur along the centerline between the fragments, or even the centerline of a single fragment, as shown in Figure 5. This is understandable in light of the asymmetry of the impacts. In cases where the critical velocity is below that of a single fragment, it is the second impact that induces the detonation. The lag in impact times enables the second fragment to sustain the initial pressure wave generated by the first fragment.

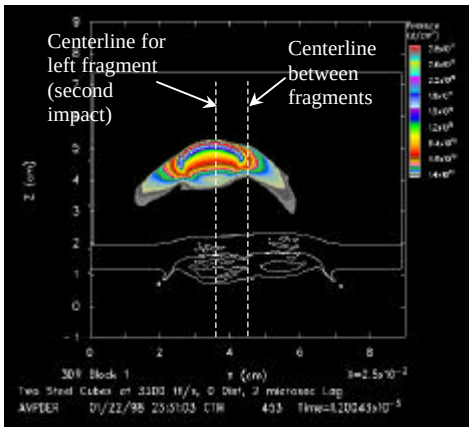

Figure 5. Asymmetric Predicted Detonation

The results of this study are shown in Figure 6. The critical velocity drops slightly below the minimum seen during the distance spacing study before rising to converge to single fragment impact velocity.

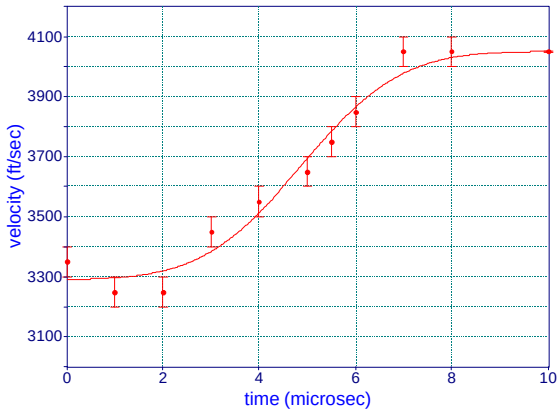

Figure 6. Summary of Zero Distance Separation Results for 250-Grain Fragments

The final step in developing the detonation threshold surface is to simultaneously vary the separation in time and in distance. These hydrocode runs yielded very interesting results, both in terms of phenomena seen and the data points to be included on the surface. Figure 7 shows some of the combined effects. In Figure 7a, the second fragment detonates first, along with the pressure wave built by the contributions from both fragments, although the first fragment (on the right) will detonate at the next time step of the run. In Figure 7b, the second fragment (on the left) causes a detonation, even though the pressure wave from the first fragment is almost completely dissipated. Figure 7c may provide some insight into the mechanism underlying the results in 7b. Here, we can see that the pressure field generated by the first fragment does not allow the pressure field generated by the second fragment to dissipate (and vice versa), thereby allowing the two-fragment system to cause the transition to detonation.

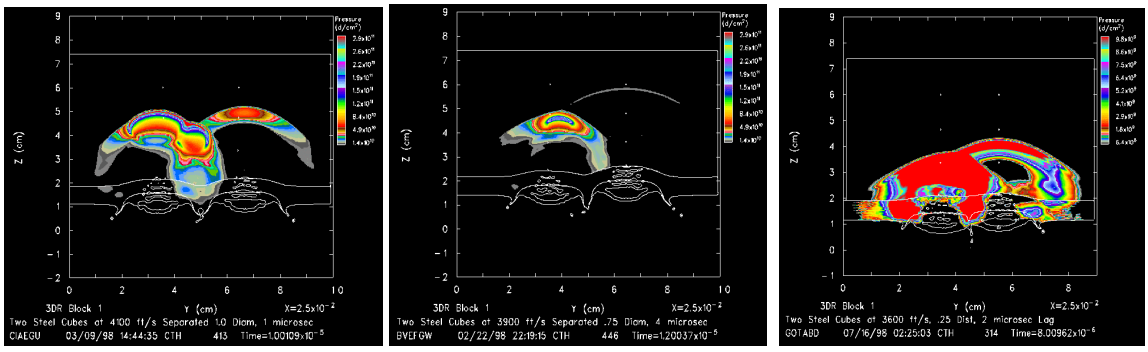

7a. 7b. 7c.

Figure 7. Some Effects of Combined Space and Time Separations

In order to fit a surface to this set of data, we used three-dimensional curve-fitting software by Jandel Scientific. Figure 8 shows the detonation threshold surface, with actual velocities, for the 250-grain fragment study. Although all the data points do not fall on the surface, the trends agree – on both axes (distance and time) the surface plateaus to the single fragment critical velocity. The surface has a local minimum that is not at the origin, which we expected due to the interactions in time.

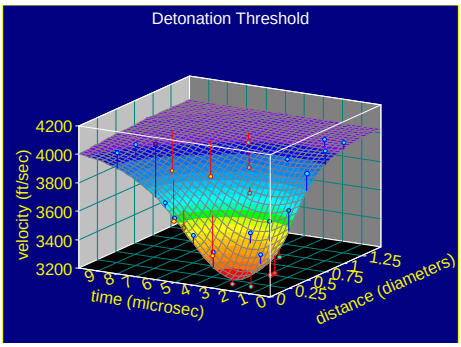

Figure 8. Detonation Threshold Surface

The normalized detonation threshold surface is identical to the surface that is shown in Figure 8, but the unitless velocity range is from zero to one. The normalized surface can be used as the scaling function for the Jacobs-Roslund equation.

Generalizing the 250-Grain Fragment Results – Comparing with 60-Grain Fragments

After developing the detonation threshold surface, the next task was to determine whether the same surface accurately describes the critical velocity of other fragment sizes and shapes. We initiated a study of 60-grain fragments, using the same explosive and cover plate thickness. The fragment dimensions were 0.318 inch (0.807 cm) by 0.318 inch by 0.3 inch (0.762 cm) thick. The square face of the fragments impacted the target. This fragment is not geometrically scaled from the 250-grain fragment, so there is variation in fragment L/d (length-to-diameter ratio). The change in critical diameter (from 0.648 inch to 0.318 inch) also causes a change in the problem T/d (ratio of target plate thickness to fragment diameter). In both cases, we kept the fragment thickness and target coverplate thickness constant, so L/d equals T/d. For the 250-grain fragment T/d approximately equals ½; for the 60-grain fragment, T/d approximately equals 1.

First, we examined the effect of distance separation for two simultaneous impacts. As can be seen in Figure 9, the smaller critical diameter (and presented area) of the 60-grain fragment significantly raises its critical velocity when compared with the 250-grain fragment.

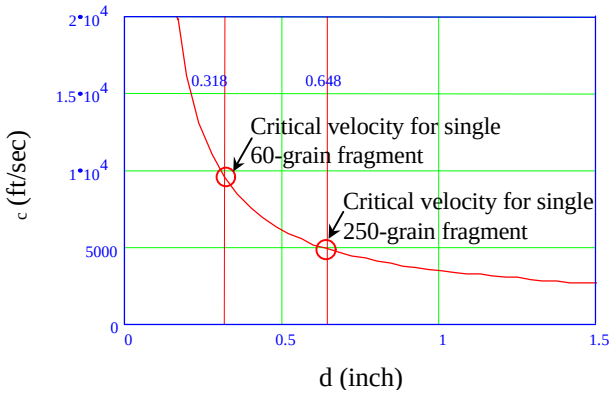

Figure 9. Jacobs-Roslund Relation Varied with Critical Fragment Diameter

The higher velocity changes the interaction of the fragment with the target coverplate and explosive. The fragment erodes the target cover and transmits a slightly different shock wave to the explosive. The wave spreads over a larger area. These effects are shown in Figure 10. As a result, the interactive effects of the impacts spread over a longer distance than for the 250-grain fragments.

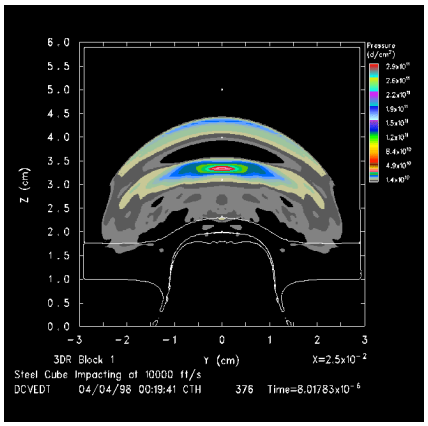

Figure 10. Shock Wave and Coverplate Erosion
Caused by 60-Grain Fragment Impact

Figure 11 shows the summarized results for zero time separation. Again, the maximum velocity matches the velocity required for a single fragment to cause a shock-to-detonation transition in the explosive. In spite of the differences in the shock wave, the equation for the curve is of the same form used for the 250-grain fragment study.

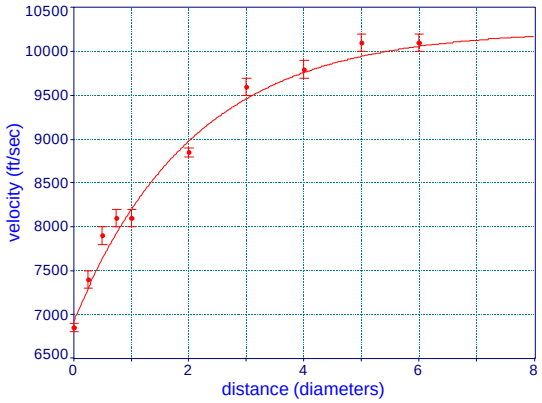

Figure 11. Summary of Zero Time Separation Results for 60-Grain Fragments

Next, we looked at the time separation. As with the 250-grain fragments, the underlying physics of the fragment-target interaction for the time-separated fragments is very different from that of the distance-separated fragments. Because of the very high speed of the fragments, the first fragment erodes through the coverplate and creates a wide crater. When the second fragment impacts at a later time, it stirkes within the crater created by the first fragment, as shown in Figure 12.

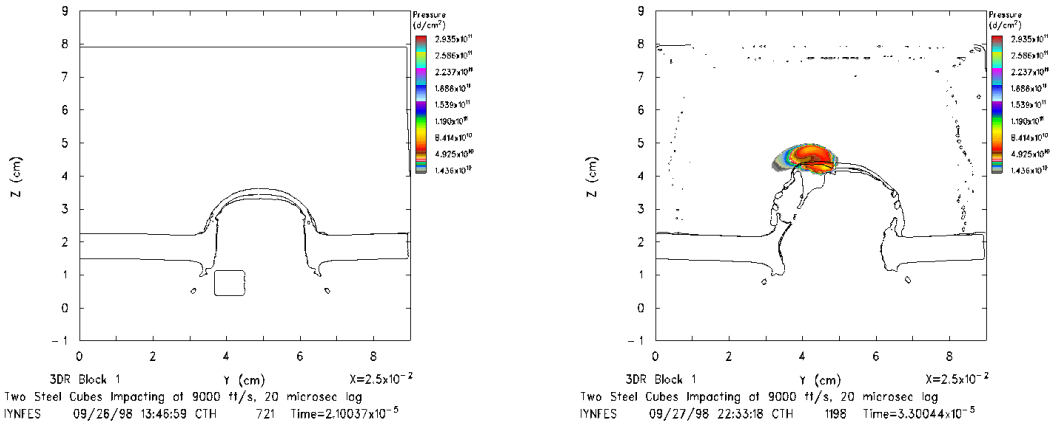

12a. 12b.

Figure 12. Fragment-Target Interaction at Large Time Separations

Because of this, the second fragment transmits a greater shock which initiates a detonation. As a result, the critical velocity does not rise to the single fragment velocity, as shown in Figure 13.

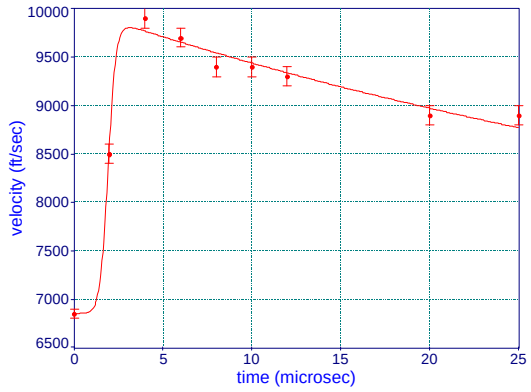

Figure 13. Summary of Results for Zero Distance Separation for 60-Grain Fragments

The equation for the curve shown in Figure 13 is not of the same form as the curve shown in Figure 6. In turn, the behavior demonstrated by the 60-grain fragments does not fit the general trends that we saw with the 250-grain fragments. For example, with increasing time, the critical velocity does not plateau to the single fragment velocity, which was one criterion used to find a fit for the 250-grain detonation threshold surface. Because of the good comparison between Figures 4 and 11, and the simplicity of the equations they follow, we decided to pursue a general solution for separation in distance. Based upon the interaction between the fragments spaced in time and their more complex equations, we determined that finding a general solution for time separations requires significantly more study. It may not be possible to generalize these results.

Pursuing a generalized equation for distance separations

The equation that fit both Figure 4 and Figure 11 is given in Equation 4.

$$V_c(s) = (a-b)\exp(-c \cdot s) + b \qquad [4]$$

where

V_c is the fragment critical velocity
s is the fragment spacing in diameters
a, b, and c are curve-fitting constants

Upon examination, it was clear that a equals the minimum critical velocity, that of two adjacent fragments hitting simultaneously. b is the maximum velocity, or single fragment critical velocity. Those two numbers could be substituted with their equivalent Jacobs-Roslund values as calculated in Table 1. However, c was not intuitively clear. It was different for each fragment size. We considered the geometries that we had varied; fragment frontal area (a function of d), fragment shape (L/d) and the coverplate thickness compared to the fragment size (T/d). The ratio T/d struck a chord because Jacobs-Roslund uses the same ratio, and because non-dimensional ratios eliminate the problem of deciding units. Because of our restrictions upon the geometry during the study, L equals T, so it could be either based upon the 250- and 60-grain studies. Looking at the values of c provided by Tablecurve, we could see that c was not a straightforward function of critical fragment diameter alone. We found that the best fit for both data sets came when we used Equation 5.

$$c = \frac{1}{C} \cdot \left(\frac{d}{T}\right)^2 \qquad [5]$$

where C is the coverplate coefficient used in the Jacobs-Roslund relation

To see whether this definition of c is true for other cases, we checked 120-grain fragments, 0.449 inch (1.14 cm) by 0.449 inch by 0.3inch. Figure 14 shows that the results match the curve very closely.

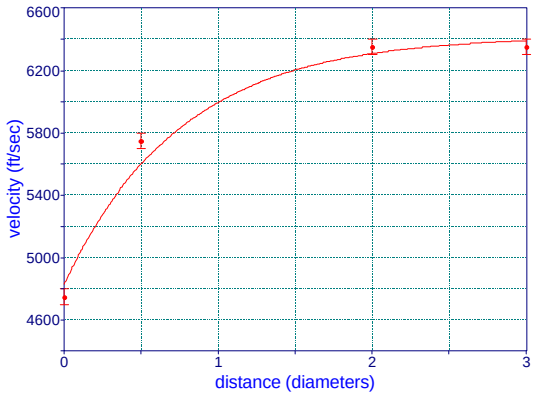

Figure 14. Summary of Zero Time Separation Results for 120-Grain Fragments

To see whether L should be used instead of T in the equation for *c*, we looked at 250-grain platelets with an L/d of about 0.1, with the same T/d as the original 250-grain fragments. At this L/d, length effects begin clouding the issues. However, Figure 15 shows that the best fit still comes from using T^2 instead of TL or L^2; the maximum velocity value and the steepness of the rise are a better match to the data.

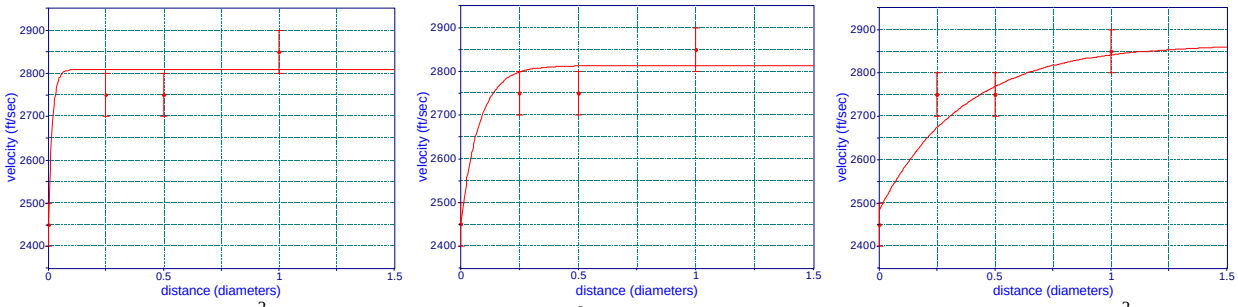

15a. Using L^2 15b. Using TL 15c. Using T^2

Figure 15. Comparing Definitions of *c*

The critical velocity equation based upon the Jacobs-Roslund relation, Equation 4, and Equation 5, is shown in Equation 6.

$$V_{c,mod} = \left[V_{JR}\left(2 \cdot A_p\right) - V_{JR}(d)\right]\exp\left(\frac{-d^2}{C \cdot T^2} \cdot s\right) + V_{JR}(d)$$

$$V_{c,mod} = A(1+B)\left\{\left[\frac{1}{(2 \cdot A_p)^{\frac{1}{4}}}\left(1+\frac{CT}{\sqrt{2 \cdot A_p}}\right) - \frac{1}{\sqrt{d}}\left(1+\frac{CT}{d}\right)\right]\exp\left(\frac{-d^2}{C \cdot T^2} \cdot s\right) + \frac{1}{\sqrt{d}}\left(1+\frac{CT}{d}\right)\right\} \quad [6]$$

where $V_{JR}(x)$ is the Jacobs-Roslund velocity using *x* as the critical fragment parameter
A_p is presented area of a single fragment ($A_p = d^2$ for a square fragment)
$V_{JR}(2\,A_p)$ is the critical velocity of two adjacent fragments, the equation minimum

In the following figures, the original Jacobs-Roslund relation is compared to Equation 6. We used the Jacobs-Rosland constants, A, B, and C, for a flat fragment into a steel cover over Comp B, as studied in the hydrocode runs. Because we are comparing a dual fragment equation with a single fragment equation, we used a spacing of 10 diameters in the dual fragment equation to simulate a single fragment. This is based upon previous study results (Figures 4, 9, 11); all the studied fragment sizes converged to single fragment velocity within 5 diameters, so interactions should be negligible at 10 diameters. Figure 16 compares the two velocity relations as a function of *d*; they begin to diverge slightly when T/d exceeds 1.5. Increasing *s* will close the gap.

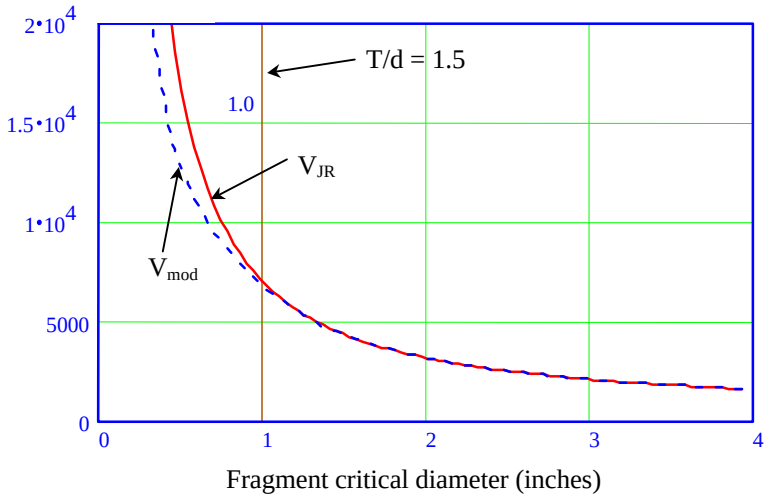

Figure 16. Critical Velocity as a Function of Fragment Critical Diameter, T = 1.5 inch, *s* = 10 diameters

Figure 17 varies the two equations with T, and it shows the same good agreement for T/d less than 1.5. Again, increasing s will decrease the discrepancy – at s = 100, Figures 14 and 15 match for T/d less than 4. T/d equal to 1.5 is near the boundary of the usefulness of Jacobs-Roslund in any case. It may be that fragment-cover geometries with T/d greater than 1.5 do cause fragments to interact at larger distances (diameters); it's beyond the scope of what we have yet studied.

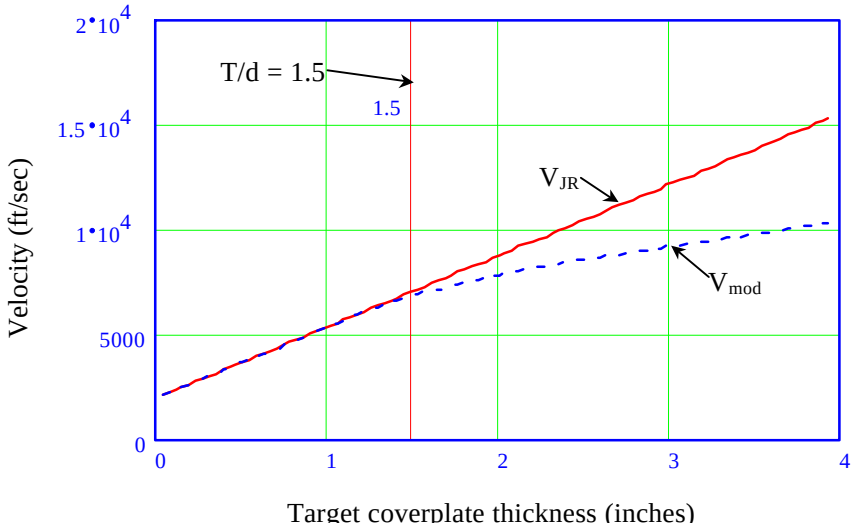

Figure 17. Critical Velocity as a Function of Target Coverplate Thickness, *d* = 1 inch, *s* = 10 diameters

Figure 18 shows how CTH results compare to both the modified velocity equation and the Jacob-Roslund velocity (V_{JR}) as a function of fragment spacing s. V_{JR} does not vary with spacing; it is single-valued for each fragment size. The modified equation accounts for fragment separation. The shapes of the curves for each fragment size (CTH results and Jacobs-Roslund-based equation) are similar. For the 60-grain fragments, CTH predicts a higher maximum velocity than Jacobs-Roslund. For the 250-grain fragments, CTH predicts a lower velocity. An

examination of the residuals, shown in Figure 19, indicates no systematic bias in the CTH results.

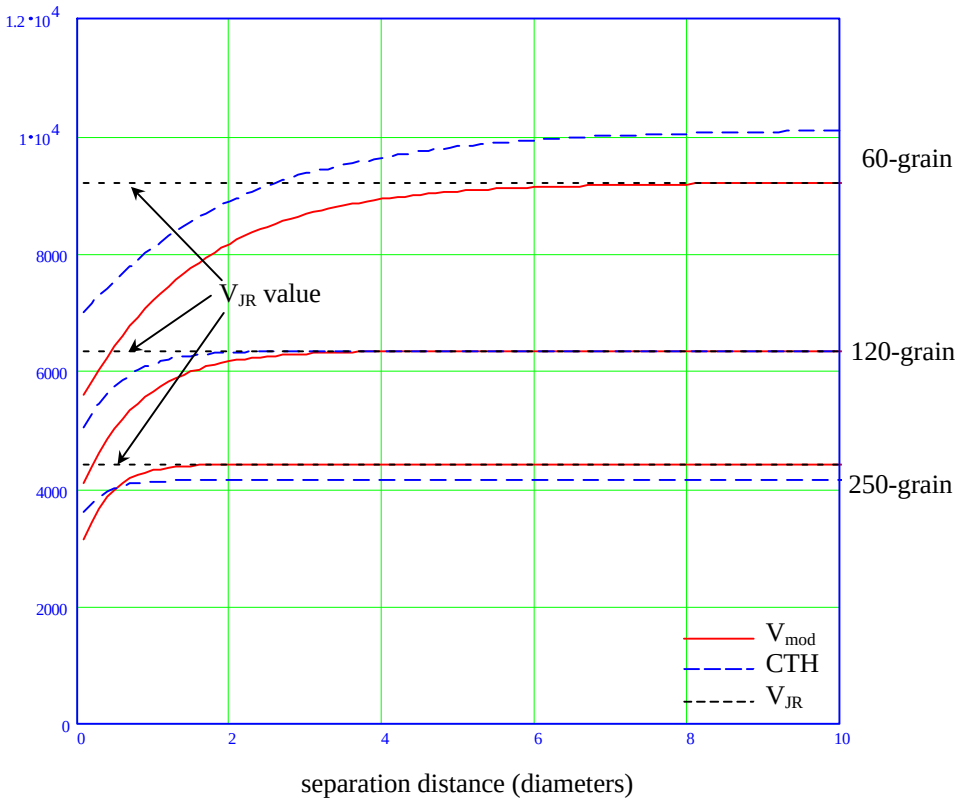

Figure 18. Comparing CTH Results with Modified Velocity Equation as a Function of Fragment Spacing

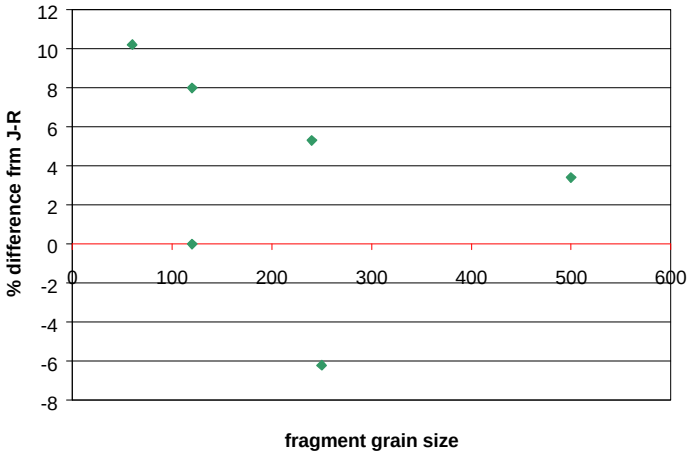

Figure 19. CTH Residuals – Variations from Jacobs-Roslund as a Function of Fragment Grain Size

CONCLUSIONS

Based upon the work shown here, the following conclusions can be reached:

1. The hydrocode CTH gives results comparable to the Jacobs-Roslund relation, making it useful for determining trends in fragment-target interaction.

2. Based upon the 250-grain fragment study, the effect of separating fragments in time can be more detrimental to the target than simply placing fragments close together in space.

3. Based upon the comparison between the 250- and 60-grain fragment time separation studies, a general critical velocity relation which accounts for variation in impact times may depend on more variables than are easily determined for or employed in an empirical relation.

4. The distance separating fragments (in the dimension parallel to the target) can significantly affect the critical velocity required to initiate a covered charge. The Jacobs-Roslund relation does not account for this effect. Equation 6 may be an appropriate alternative.

ACKNOWLEDGEMENTS

We appreciate the support and funding we received from David Wilson, Lori Chrysostom and William Hoffman of NSWC Carderock Division. We also thank Jeanette and Jennifer Dickens for their editing and production assistance.

REFERENCES

1. Dickinson, David and Wilson, Leonard T., *The Effect of Impact Orientation on the Critical Velocity Needed to Initiate a Covered Explosive Charge,* EMI HVIS, Freiburg i. Br., Germany, October 7-10, 1996

2. Hertel, E.S.; Bell, R. L.; Elrick, M. G.; Farnsworth, A. V.; Kerley, G. I.; McGlaun, J. .M.; Petney, S. V.; Silling, S. A.; Taylor, P. A. and, Yarrington, L., *CTH: A Software Family for Multi-Dimensional Shock Physics Analysis,* Proceedings of the 19th International Symposium on Shock Waves, Volume 1, pages 377-382, Marseilles, France, 26-30 July 1993

3. Hertel, Eugene S. and Kerley, Gerald I., *CTH Reference Manual: The Equation of State Package,* SAND98-0947 UC-705, Sandia National Laboratories, EXPORT CONTROLLED Jacobs-Roslund

4. TableCurve 2D v4.0 software © Copyright 1996, 1994, 1992, 1991, 1990 and 1989 AISN Software, Inc., All Rights Reserved and TableCurve 2D v4.0 Documentation © Copyright 1996 AISN Software, Inc.

5. TableCurve 3D v1.0 Software and User's Manual, © Copyright 1993 AISN Software, Inc.